

## P2.4 VALIDATION OF CERES/SARB DATA PRODUCT USING ARM SURFACE FLUX OBSERVATIONS

David Rutan<sup>1</sup>, Tom Charlock<sup>2</sup>, Fred Rose<sup>1</sup>, Nitchie Manalo-Smith<sup>1</sup>

<sup>1</sup>Analytical Services & Materials Inc., Hampton, VA

<sup>2</sup>NASA Langley Research Center, Hampton, VA

### 1 INTRODUCTION

This paper uses surface observed broadband fluxes from around the globe to validate surface flux model results from the Clouds and the Earth's Radiant Energy System (CERES) Surface and Atmospheric Radiation Budget (SARB) Clouds & Radiative Swath (CRS) data products during the months Jan-Dec 2001. CERES instruments fly aboard the Terra and Aqua satellites measuring broadband radiation in three channels: total (0.3-∞ μm), shortwave (0.3-5.0 μm) and window (8-12.0 μm) at the Top Of the Atmosphere (TOA). The CRS product supplies, along with CERES observed fluxes, model calculated fluxes at five atmospheric levels beneath every other CERES footprint. The radiation transfer code used is a modified version of the Fu & Liou model and is described in more detail below. CERES observations supply a "truth" against which the model can be compared at the TOA and broadband surface flux observations provide the same at Earth's surface. Results are encouraging in that all-sky biases, including all sites, for downward longwave (LW) and shortwave (SW) flux are less than 2%. For clear sky biases are less than 1% for SW, less than 3% for LW. The worst error occurs in SW insolation under overcast skies with biases approaching 7%. These biases and their associated RMS' vary geographically as will be shown below.

### 2 SURFACE FLUX OBSERVATION (ARM, SURFRAD, CMDL, BSRN, NREL, LaRC)

Surface observations used in this study include 40 sites worldwide. Listed in Table 1, they were selected due to adherence to Baseline Surface Radiation Network standards (Ohmura et al 1998.) Table 1 also shows pertinent web sites and references for each set of surface data. Most sites are in fact BSRN sites though much of the data is generously supplied to SARB before it enters the BSRN archive. Upwelling and downwelling surface observations of

irradiance are generally made from 10m towers and reported as one-minute averages. For SW insolation we preferentially choose "total" insolation (direct normal radiation + diffuse) if available. If the total observation is un-available a global (unshaded PSP) observation is used. For SARB validation these data are averaged to 30-minute time steps along with other surface meteorological variables available at each site. These 30-minute average data files (one file per month per site) along with on-line plotting capabilities, are made available via the CERES/ARM Validation Experiment (CAVE) web site: <http://www-cave.larc.nasa.gov/cave>.

### 3 RADIATION TRANSFER MODEL

The radiation transfer model used in SARB is a modified version of the Fu & Liou (1993) code. It is a delta-two stream (2 for SW, 2/4 for LW) radiation transfer code with fifteen spectral bands from 0.175 to 4.0 μm in SW and twelve LW spectral bands between 2850 and 0 cm<sup>-1</sup>. Cloud properties are given by MODIS imager pixels collocated within larger CERES footprints. Aerosol optical depths are input from MODIS (MOD08D3) product. The Collins/Rasch Model of Atmospheric Transport and CHemistry (MATCH) model defines aerosol constituents (Collins et al 2001) and scale heights. Aerosol optical depths from MATCH are used where the MODIS product is un-available (often over desert regions) or cloud fraction is greater than 75% (often over polar regions.) Actual aerosol properties (single scatter albedo, scattering coefficient etc...) are given by matching seven aerosol types from the MATCH model to aerosol properties given by Hess et al. (1998) and Tegen and Lacis (1996). Pressure, temperature, and water vapor profiles are specified from GEOS-4.0 and ozone from NCEP's, Stratospheric Monitoring Group Ozone Blended Analysis (SMOBA) product from SBUV & TOVS.

Surface albedo comes from a number of different sources. Surface albedo over ocean is available from a lookup table based on the Coupled Ocean/Atmosphere Radiation Transfer (COART) model of Jin (2002). Over clear sky land, surface albedo is derived from a TOA to surface parameterization. Clear sky surface albedos are pre-processed for a month saving the minimum value in

---

Corresponding Author:

David A Rutan ([d.a.rutan@larc.nasa.gov](mailto:d.a.rutan@larc.nasa.gov))

1 Enterprise Pkwy Suite 300

Hampton, VA 23666

an equal angle, 10-minute resolution grid. This “history” map is used to supply broadband albedo under cloudy footprints. If no clear sky is available a climatological value is used. Albedo spectral shapes come from a scene type (IGBP) based lookup table.

The radiation transfer model is run eight times for each footprint. These runs include a pristine (no clouds or aerosols), clear (no clouds), cloudy pristine (include clouds, no aerosols) and an all-sky run. These four conditions are run twice, one untuned and one tuned run. For the all sky run, CERES fluxes are assumed a “truth” against which the model can be compared. Hence, the model is run with its initial inputs (untuned) and TOA model flux is compared with CERES observations. Certain input parameters, depending on atmospheric conditions, are then

modified using a Lagrange Multipliers minimization technique. Each possible tunable parameter is assigned a “sigma”, an estimate of quality of that particular variable, which constrains the adjustment process not allowing any one variable to “move” too much. Similar error estimates are assigned to TOA fluxes so that exact matches of model and observed TOA fluxes are not required. For example under clear skies, for shortwave flux, aerosol optical depth and surface albedo can be “tuned” to better match observed TOA flux. Only a single iteration is computed. Constraining the model to CERES observations at TOA leaves surface fluxes to change depending on what is required for a better match at the top.

| Project   | Sponsor           | # Sites | Web Link   | Reference:            |
|---|-------------------|---------|--|-----------------------|
| ARM SGP/TWP   | DOE <sup>1</sup>  | 22      | <a href="http://www.arm.gov">www.arm.gov</a>   | Acknowledgements      |
| CMDL  | NOAA <sup>2</sup> | 6       | <a href="http://www.cmdl.noaa.gov">www.cmdl.noaa.gov</a>   | Acknowledgements      |
| SURFRAD   | NOAA <sup>2</sup> | 6       | <a href="http://www.srnb.noaa.gov">www.srnb.noaa.gov</a>   | Augustine et al. 2000 |
| BSRN  | WCRP <sup>3</sup> | 4       | <a href="http://www.ethz.ch">www.ethz.ch</a>   | Ohmura et al. 1998    |
| NREL  | DOE <sup>4</sup>  | 1       | <a href="http://rredc.nrel.gov/solar/new_data/Saudi_Arabia">rredc.nrel.gov/solar/new_data/Saudi_Arabia</a> | Myers et al. 1999     |
| NASA LaRC   | NASA <sup>5</sup> | 1       | <a href="http://www-svg.larc.nasa.gov">www-svg.larc.nasa.gov</a>   | Jin et al. 2002       |
| <ol style="list-style-type: none"> <li>1. Atmospheric Radiation Measurement Program, Department of Energy</li> <li>2. Climate Monitoring Diagnostics Laboratory, National Oceanic and Atmospheric Administration</li> <li>3. Baseline Surface Radiation Network, World Climate Research Programme</li> <li>4. National Renewable Energy Laboratory, Department of Energy</li> <li>5. NASA Langley Research Center, National Aeronautics and Space Administration</li> </ol> |                   |         |  |                       |

Table 1. Surface sites, associated web pages, and referencing information.

#### 4 MODEL/DATA COMPARISONS

As stated above, downwelling and upwelling surface observations of LW and SW irradiances are averaged to ½hour means and collected for each month at each site. As CERES sweeps past a surface site contained in the CAVE database, the centroid of each footprint is located with respect to the surface site. Within a given half hour only the footprint that comes closest to a surface site (footprint centroid no greater than 15km away) is retained for comparison with surface observations. To account for differences in solar zenith angle within the ½hour flux averages, a surface flux observation is adjusted by the ratio of the surface 30 minute average solar zenith angle and

footprint solar zenith angle at the satellite observation time. Clear skies are determined within the CERES footprint by collocation of satellite imager pixels within the larger CERES footprint. A secondary check for cloud fraction is specified by the Short Wave Flux (SWF) cloud fraction as given by the Long and Ackerman (2000) cloud fraction algorithm. Tables that include SWF cloud fraction are found at the CAVE website. Results shown here are subset by “all sky”- all footprints, “clear sky”- CERES cloud fraction equal to 0.0, and “overcast” – CERES cloud fraction equal to 1.0. CAVE sites are grouped by geographic region as shown in Table 2 and their surface biases are shown in Table 3.

| Region | Central USA      | Polar  | Island                                  | North America   | Coastal          | ALL                                      |
|--------|------------------|--|---|-----------------|------------------|--|
| Sites  | 20 ARM/SGP sites | South Pole, G. Von Neumeyer, Syowa, Barrow, AK | Manus, Nauru, Kwajalein, Bermuda, Samoa | 6 SURFRAD sites | Tatano, JP, COVE | All sites except only 5 ARM/SGP included |

Table 2. Surface sites contained in each geographic region.

Table 3 gives a comprehensive summary of downward LW and SW surface flux bias and RMS for each geographic region and for 'All' CAVE sites, for Jan. through Dec. 2001. (In this table and in Figure 1, we do not in fact include all the surface sites available. We exclude all but 5 ARM/SGP sites since using all 20 SGP sites skews statistics towards central North America.) The sense of the bias is model minus observation. Hence negative LW implies too cool an atmosphere and positive shortwave implies the model is too transmissive. Recall these numbers are for instantaneous

comparisons, not daily averages, subsequently LW does represent day and night footprints. A daily average bias for SW would be halved from the numbers shown. Figure 1 shows a comparison of model and observed downwelling LW and SW fluxes at the same 28 surface sites for 2001. Black, red, and blue indicate overcast, partly cloudy, and clear sky footprints respectively. This is an example of plots available at all surface sites in the CAVE database at <http://www-cave.larc.nasa.gov/cave/valplot/>.

| Downward Surface Flux (Tuned Model-Obs) Bias(RMS) (W/m <sup>2</sup> ) |          |           |           |           |
|---|----------|-----------|-----------|-----------|
|   | All Sky  |           | Clear Sky |           |
|   | Longwave | Shortwave | Longwave  | Shortwave |
| ARM/SGP   | -9(17)   | 7(76)     | -11(15)   | 3(19)     |
| Island Sites  | -4(14)   | 39(150)   | -4(11)    | 7(44)     |
| Polar Sites   | 1(29)    | -1(66)    | -9(15)    | -8(21)    |
| SURFRAD   | -7(20)   | 11(93)    | -8(17)    | -2(22)    |
| Coastal   | 3(19)    | 24(93)    | 4(12)     | -5(33)    |
| ALL*  | -4(23)   | 9(93)     | -8(17)    | -6(32)    |

Table 3. Surface SW & LW bias CERES/SARB tuned CRS (model) results minus surface observations.

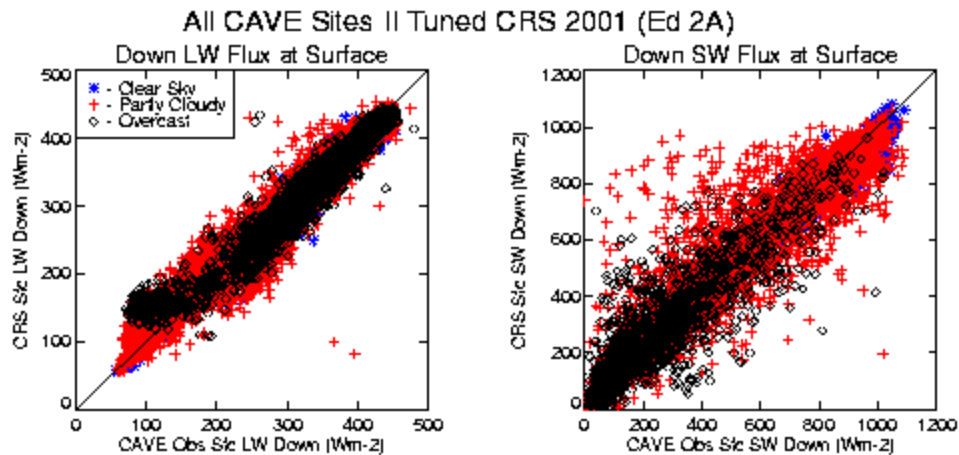


Figure 1. Comparison of CRS and surface observed downwelling LW and SW radiation at 28 CAVE sites during 2001.

More detailed tables of statistics for each site along with aerosol and cloud forcing are given with each plot at the above web site. A summary of TOA and surface bias statistics for both tuned and untuned

results is shown in Table 4. Flux comparisons at TOA are shown in gray, surface fluxes in white. For each cloud condition both untuned and tuned results are shown. Recall that the model is constrained by

| CAVE Sites |        | TOA & Surface Model-Observed Bias (RMS) ( $W/m^2$ ) |         |           |         |          |         |
|------------|--------|---|---------|-----------|---------|----------|---------|
|            |        | All Sky   |         | Clear Sky |         | Overcast |         |
|            |        | Untuned   | Tuned   | Untuned   | Tuned   | Untuned  | Tuned   |
| LW         | TOA Up | 1(9)  | 1(5)    | -1(5)     | -1(3)   | 1(11)    | 1(4)    |
|            | Sfc Dn | -4(23)  | -4(23)  | -8(17)    | -8(17)  | -3(23)   | -3(24)  |
|            | Sfc Up | -4(25)  | -4(23)  | -1(20)    | -1(20)  | 2(21)    | 2(21)   |
| SW         | TOA Up | 4(27)   | 1(12)   | 2(7)      | 1(3)    | 5(33)    | -2(17)  |
|            | Sfc Dn | 8(91)   | 9(93)   | -6(32)    | -6(32)  | 9(99)    | 19(104) |
|            | Sfc Up | -19(56)   | -19(56) | -19(35)   | -20(35) | -17(59)  | -16(59) |

Table 4. Biases and RMS' for TOA and surface comparisons at 28 CAVE sites for all of 2001. Biases indicate model minus observations for both constrained and unconstrained model runs, subset by cloud condition.

the TOA comparison. This is evident by a reduction in bias and RMS under all cloud conditions at TOA from untuned to tuned results. Surface fluxes are left to react to changes in model inputs as determined by the tuning algorithm. In general this does not affect surface flux comparisons significantly. One exception is surface SW insolation under overcast skies. There one finds an initial TOA SW error of  $5 W/m^2$  and RMS of  $33 W/m^2$ . The tuning algorithm assumes clouds are too reflective, subsequently reducing either cloud amount or cloud optical depth or both. TOA error is reduced to  $-2W/m^2$  bias and  $17 W/m^2$  RMS. However, reducing either cloud amount or optical will increase flux observed at the surface hence increasing the relative difference. This is seen in Table 4 where a positive bias of  $9 W/m^2$  increases to  $19 W/m^2$ . This error in TOA reflected SW radiation has been found to be worse over oceans and is partly responsible for the large insolation errors seen in the all sky SW biases at "Island" and "Coast" groups in Table 3.

Successes are found in these results in TOA upward fluxes, the effect of the tuning algorithm to reduce RMS at TOA, and clear sky surface insolation results. Also in LW up at the surface, which is a proxy for surface skin temperature, biases are small. Besides overcast SW insolation another primary problem seen in the tables is a mismatch of upward surface SW flux. This is due to a spatial mismatch in surface albedos. The CERES footprint is approximately 20km long in a nadir viewing position and this spatial extent increases with increasing viewing zenith angle. Since most sites have downlooking radiometers at 10m albedos can only match if the few square meters viewed by the downlooking radiometer approximates that of the surrounding 20 to 50 square kilometers.

## 5 AEROSOL and CRS

Aerosol optical thickness (AOT) is input into the CRS code from three primary sources, MODIS

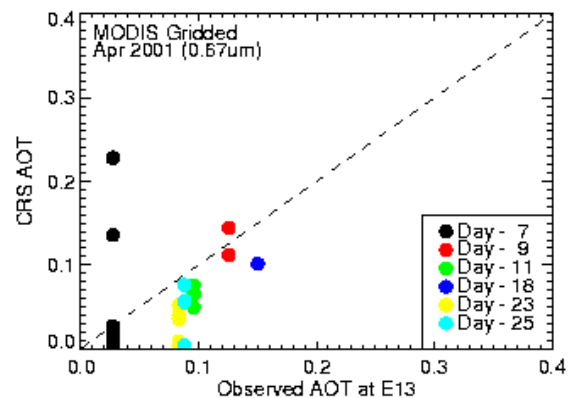


Figure 2. MODIS gridded aerosol optical thickness used for each footprint vs. either AERONET or MFRSR AOT observation within that same 1/2hour for days in Apr. 2001.

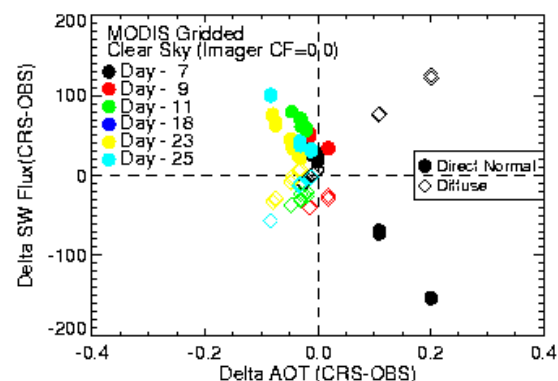


Figure 3. CRS Direct normal and diffuse SW flux differenced from observed fluxes at ARM/SGP site E13, versus, MODIS gridded AOT differenced from surface observed AOT. Points in plot correspond to aerosol shown in Figure 2

instantaneous retrievals, MODIS gridded data, and the MATCH model as described in section 3 above. The MATCH model always defines aerosol constituents. The primary AOT source under clear skies is MODIS instantaneous though often MODIS

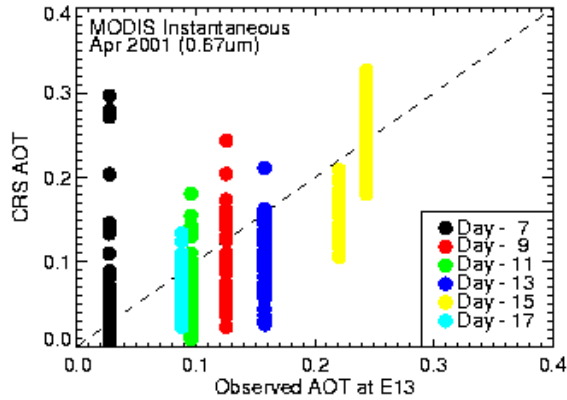


Figure 4. MODIS instantaneous aerosol optical thickness used for each footprint vs. either AERONET or MFRSR AOT observation within that same 1/2 hour for days in Apr. 2001.

gridded is substituted when there is no instantaneous solution, often due to a glint. To show the effect of input aerosol on CRS calculations footprints were isolated within 115km of the ARM Central facility in Oklahoma during April 2001 under clear skies and when there was a surface observed estimate of AOT. (Surface observed AOT was interpolated in time if there were at least two surface observations during the day.) Results are shown in two ways. First, Figure 2 shows a direct comparison of AOT (MODIS Gridded only) used in CRS and that observed at the surface (AERONET or MFRSR). There one finds, for these days, CRS AOT generally underestimates surface observations. The effect of this on SW insolation is shown in Figure 3. For example, when CRS aerosol is lower than observed, direct normal flux (solid circles) tends to be too high while diffuse (open diamonds) is too low. For the few points where CRS AOT is greater than that observed it has the opposite effect on the direct and diffuse insolation. Ideally as the difference of surface observed and CRS AOT goes to zero error in the direct and diffuse flux goes to zero. “Eyeballing” regression lines through the direct and diffuse points indicates this is not always the case, particularly on April 9<sup>th</sup>. In general direct and diffuse errors tend to cancel, though not entirely. To increase the sample we use footprints less than 115km away from E13. This can cause spatial mismatches given spatial gradients in aerosols that day.

Figures 4 and 5 show similar results as Figures 2 and 3 except for clear sky CRS calculations that used MODIS instantaneous data. Note that several days used both gridded and instantaneous values within the same area near the same time. Again, in Figure 4 the MODIS tends to underestimate surface observations and Figure 5 shows similar behavior of

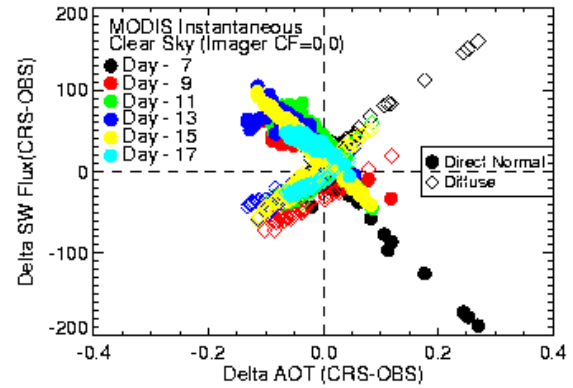


Figure 5. CRS Direct normal and diffuse SW flux differenced from observed fluxes at ARM/SGP site E13, versus, MODIS instantaneous AOT differenced from surface observed AOT. Points in plot correspond to aerosol shown in Figure 4.

direct and diffuse radiation. Too on most days it appears that as the difference between observed and MODIS AOT goes to zero SW error also moves towards zero.

The importance of having accurate AOT for CRS calculations is manifest when calculating aerosol forcing. This is done in CRS results in that the code is run for both pristine (no aerosol) and cloud free conditions allowing calculation of aerosol forcing to clear skies. In the mean for the year 2001, at E13, clear sky SW bias (for footprints within 15km) is  $3. W/m^2$  and aerosol forcing at the surface for those same footprints is  $-16 W/m^2$ . (Validation table available at:

<http://www-cave.larc.nasa.gov/cave/valplot/>.) With the addition of MODIS aerosols and MATCH model aerosols and constituents for CRS edition 2a, figures 2 through 5 add confidence to CRS aerosol forcing results as the RMS is reduced by multiple observations over long periods of time.

## 6 ACKNOWLEDGMENTS

ARM data is made available through the US Department of Energy as part of the Atmospheric Radiation Measurement Program. CMDL data is made available through the NOAA/CMDL Solar and Thermal Radiation (STAR) group. SURFRAD data is made available through NOAA's Air Resources Laboratory/Surface Radiation Research Branch. COVE data is made available through NASA Langley Research Center's, Atmospheric Sciences Competency, CERES Surface and Airborne Radiometry Calibration group. CERES data is made available from NASA Langley's Atmospheric Sciences Data Center at <http://eosweb.larc.nasa.gov/>.

We thank the PI for AERONET data at the ARM Central Facility (CART Site), Mary Jane Bartholomew, for making this valuable data available. Also we thank SUNY Albany ASRC Solar Group for supplying total optical depths from an MFRSR maintained at the CART site.

## 7 REFERENCES

- Augustine, J. A., J. J. DeLuisi, and C. N. Long, 2000: SURFRAD-A National Surface Radiation Budget Network for Atmospheric Research, *Bull. Of Amer. Met. Soc.* Vol. 81, No. 10, pp. 2341-2358.
- Collins, W.D., P.J. Rasch, B.E. Eaton, B.V. Khattatov, J.-F. Lamarque, and C.S. Zender, 2001: Simulating aerosols using a chemical transport model with assimilation of satellite aerosol retrievals Methodology for INDOEX. *J. Geophys. Res.* **106**, 7313-7336.
- Fu, Q., and K.N. Liou, 1993: Parameterization of the radiative properties of cirrus clouds. *J. Atmos. Sci.*, **50**, 2008-2025.
- Hess, M.P., P. Koepke, and I. Schult, 1998: Optical properties of aerosol and clouds: The software package OPAC. *Bull. Amer. Meteor. Soc.*, **79**, 831-844.
- Jin, Z., T.P. Charlock, and K. Rutledge, 2002: Analysis of broadband solar radiation over the ocean surface at COVE, *J. Atmos. Ocean Tech.*, **19**, 1585-1601.
- Myers, D. R., S. Wilcox, M. Anderberg, S. H. Alawaji, N. M. Al Abbadi, M. Y. bin Mahfoodh, 1999: Saudi Arabian solar radiation network of data for validating satellite remote-sensing systems, *Earth Obs. Sys. IV SPIE Vol 3750*, 18-20 July, Denver CO.
- Ohmura A., E. Dutton, B. Forgan, C. Frohlich, H. Gilgen, H. Hegne, A. Heimo, G. Konig-Langlo, B. McArthur, G. Muller, R. Philipona, C. Whitlock, K. Dehne, and M. Wild, 1998: Baseline Surface Radiation Network (BSRN/WCRP): New precision radiometry for climate change research. *Bull. Amer. Meteor. Soc.*, Vol. 79, No. 10, 2115-2136.
- Rutan, D. A., F.G. Rose, N. Smith, and T. P. Charlock, 2001: Validation data set for CERES Surface and Atmospheric Radiation Budget (SARB), *WCRP GEWEX Newsletter*, **11**, No. 1, 11-12.
- Tegen, I., and A.A. Lacis, 1996: Modeling of particle size distribution and its influence on the radiative properties of mineral dust aerosol. *J. Geophys. Res.*, **101**, 19,237-19,244.
- Wielicki, B.A., B.R. Barkstrom, E.F. Harrison, R.B. Lee, G.L. Smith, and J.E. Cooper, 1996: Clouds and the Earth's Radiant Energy System (CERES): An Earth Observing System Experiment. *Bull. Amer. Meteor. Soc.*, **77**, 853-868